IJE TRANSACTIONS B: Applications Vol. 34, No. 11, (November 2021) 2433-2441

International Journal of Engineering

Journal Homepage: www.ije.ir

Design and Modeling of a High-speed Permanent Magnet Synchronous Generator with a Retention Sleeve of Rotor

H. Parivar*, A. Darabi

Department of Electrical Engineering, Shahrood University of Technology, Shahrood, Iran

PAPER INFO

Paper history:
Received 31 May 2021
Received in revised form 14 September 2021
Accepted 23 September 2021

Keywords:
high-speed Permanent Synchronous Machine
Retention Sleeve
Taguchi Optimization Method
Titanium Sleeve

ABSTRACT

In this paper, the authors present a novel approach to design a high-speed permanent magnet synchronous generator (HS-PMSG) with a retention sleeve. The importance of the retention sleeve becomes conspicuous when the rotor suffers from the radial and tangential stresses derived from a high speed say 60 krpm. With respect to the mechanical property of Titanium. This material has been demonstrated that it could be a proper material for the retention sleeve. The investigations in this paper concentrated on the electromagnetic coupled with mechanical design of a 2-poles, 18-slots, 40 KW HS-PMSG which is carried out through FEM analysis using JMAG 17.1 and ABAQUS CAE and optimized through the well-known Taguchi optimization method. The obtained results assure the robust mechanical behaviour of the HS-PMSG at a rotational speed of about 60 krpm meanwhile the cogging torque, the Joule loss, and the total weight of the optimally designed HS-PMSG were reduced 44.71, 27.87, and 2.78%, respectively compared with the initial design.

doi: *10.5829/ije.2021.34.11b.07*

1. INTRODUCTION

In the last century, electrical energy has become an undeniable part of human life. Without electrical energy, our world drowns in the darkness, modernization would be stopped and numerous consequences would threaten the life of the earth. The generation of electrical energy plays a vital role in power systems. Among all generator units, PMSGs have been utilized as a significant part of generation units. Due to the important role of PMSGs, multi1ple studies have dedicated their effort to analyze the behavior, modelling, simulation, and operation improvement of these devices [1]. They have drawn massive attention exceedingly in both low speed and high-speed industrial applications as a generator or motor. High-power density, low manufacturing costs, which is a consequence of the overall weight and the size reduction, are the advantages of the mentioned machines. Two kinds of interior PM (IPM) and surface-mounted PM (SPM) machines are becoming candidates in high-speed applications. Figure 1 represents the most important advantages and disadvantages of the PMSGs [2-6]. In the last decade and along with the discovery of new PMs, these types of generators have drawn lots of attention, not only in academic papers but also in the power engineering world [7]. Among high-speed machines, the HS-PMSGs have been utilized more widely than others. Thus, the proper design of these machines is an inevitable step in the utilization of them. The main issue in the design of such generators is to design the exact mechanical behavior of rotors considering electrical, magnetic, mechanical, thermal, and even economic aspects [8]. Protection of the PMs against the massive induced centrifugal forces of the rotor is the main objective of the design of HS-PMSGs which is dealt with by taking the advantage of retention sleeves. The aforementioned sleeves should not only have a proper mechanical resistance, suitable thermal conductance, and low electromagnetic loss but also should be thin enough [9]. The design procedure of HS-PMSG faces numerous challenges and hindrances. The mechanical stresses of the rotor, temperature

*Corresponding Author Institutional Email: hosseinparivar72@yahoo.com (H. Parivar)

Please cite this article as: H. Parivar, A. Darabi, Design and Modeling of a High-speed Permanent Magnet Synchronous Generator with a Retention Sleeve of Rotor, International Journal of Engineering, Transactions B: Applications, Vol. 34, No. 11, (2021), 2433-2441

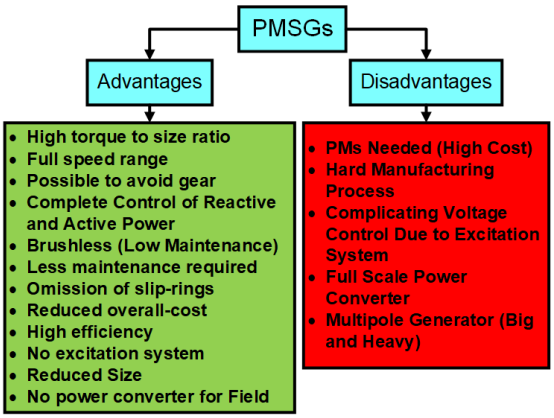

Figure 1. Advantages and disadvantages of the PMSGs [2-6]

considerations, and losses are the most significant challenges [10-11]. All the parameters affecting the mechanical and electromagnetic performance of the HS-PMSG can be determined optimally by the Taguchi optimization method. Moreover, the Taguchi optimization method is generally preferred to others such as trial and error due to faster response. In this regard, the Taguchi optimization approach is employed in this paper for designing an HS-PMSG optimally getting started from an initial design with numerous parameters. In fact, without using this optimization method, in the design process of the HS-PMSG, it is necessary to suggest various and infinite parameters for the thicknesses of the retention sleeve and the PM, while in this approach, the proper and optimum value is determined with fewer steps.

In this paper, the authors try to propose an optimum design of the HS-PMSG with a retention sleeve. The optimization process is conducted based on the well-known Taguchi optimization method which is accomplished to designate the proper thickness of PMs and retention sleeve.

The rest of this paper includes sections 2 and 3, which covered the HS-PMSG electromagnetic and mechanical modelling, respectively. The subject of section 4 is the thicknesses of the sleeve and PM. Section 5 involves results and discussions. Section 6 presents the final electromagnetic and mechanical design of HS-PMSG, and the conclusion are expressed in section-7.

2. HS-PMSG ANALYTICAL MODELING

In this section, the design approach of a HS-PMSG is presented. At first, let us start to design an instance HS-PMSG which is presented by Damiano et al. [12]. It is a 40^{KW}, 60^{krpm}, 2-pole, and 18-slot with material properties summarized in Table 1. Determining the air gap sizes can be a starting point of the machine design. In the electromagnetic design of the HS-PMSG, the retention sleeve plays a role as an extra air gap. So, the physical air gap is considered 1^{mm} which for a machine with the stated size and power, regarding previous experiences, this value of the air gap is reasonable. Analytical design of the HS-PMSG start by assuming initial design parameters like as: D: stator diameter on the airgap side = 77^{mm}, L: machine axial length = 80^{mm}, h_m: PM thickness in the radial direction = 3^{mm}. These extents are taken from a similar size and power rating machine. Owing to Figure 2, the effective air gap (g') is defined as:

$$g' = g_1 + g_2 = g + (h_m/\mu_r) = 1 + (3/1.05) = 3.85^{mm} \quad (1)$$

where μ_r is the permeability of the PM. Owing to the considered air gap size (g), the rotor radius on the air gap side (R_m) and the rotor core outer radius (R_r) are defined [13]:

$$R_m = (D/2) - g = (77/2) - 1 = 37.5^{mm} \quad (2)$$

$$R_r = R_m - h_m = 37.5 - 3 = 34.5^{mm} \quad (3)$$

The slot pitch (τ_t) and the Karter coefficient (K_c) could be conducted by Say [13]:

$$\tau_t = (2\pi R_s)/(N_s) \quad (4)$$

$$K_c = (\tau_t)/(\tau_t - \gamma g') \quad (5)$$

where R_s is the stator core inner radius and N_s is the number of stator slots. Experience shows which for a medium-sized machine (1^{KW} to 100^{KW}), the stator slot opening at the slot tip parameter (B_{s0}) is usually 2^{mm} to 3^{mm}, and the γ constant is defined as follows [13]:

$$\gamma = \frac{4}{\pi}\left(\frac{B_{s0}}{2g'}\right)\tan^{-1}\left(\frac{B_{s0}}{2g'}\right) - \ln\sqrt{\left(1+\left(B_{s0}/2g'\right)^2\right)} \quad (6)$$

Therefore, according to Equations (4) and (5) τ_t and K_c are 13.43^{mm} and 1.012, respectively. The effective stator inner radius is 38.54^{mm} evaluated by [13]:

$$R_{se} = R_s + (K_c - 1)g' \quad (7)$$

The fundamental component of back EMF (E_1) for the number of turns per phase of the stator winding given as $Nc=30$ is 292.5^{V} [13]:

$$E_1 = 4.44\, f N_c B_1 k_{w1} (2/\pi)(\pi D/p\, L) \quad (8)$$

B_1 is the fundamental spatial harmonic component of the airgap flux density produced by the PM (T), k_{w1} is the fundamental winding factor and p is the number of the poles. Therefore, the winding current is

TABLE 1. HS-PMSG Parameters

Type	Material
Stator Core	VACOFLUX-48
PMs	NdFeB NEOREC 50H (TDK)
Windings	Copper
Insulation Class	Class-F
Sleeve	Titanium

$I_{ph}=P_{out}/n_{phase}\times E_1=26.31^{A}$. The stator tooth width (T_{sw}), the stator core thickness (T_{sc}), and the rotor core thickness (T_{rc}) which are shown in Figure 2 are equal to 12.5^{mm}, 12.5^{mm}, and 3.11^{mm}, respectively [13].

$$T_{sc}=\Phi/\left(2B_{sc}Ll_f\right) \tag{9}$$

$$T_{rc}=\Phi/\left(2B_{rc}Ll_f\right) \tag{10}$$

$$T_{sw}=\Phi_{tm}/\left(B_{st}Ll_f\right) \tag{11}$$

where Φ is the flux per pole (Wb), and Φ_{tm}, B_{sc}, B_{rc}, B_{st}, and l_f are the maximum stator tooth flux (Wb), flux density in the stator core (T), flux density in the rotor core (T), flux density in the stator tooth (T) and lamination

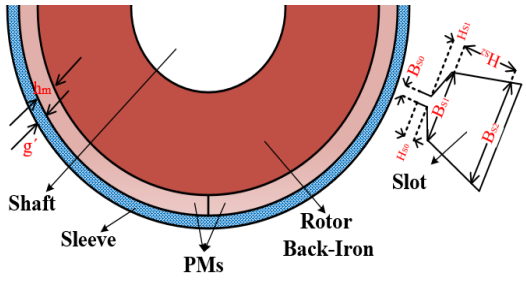

Figure 2. The design parameters of HS-PMSG

TABLE 4. The PM and sleeve thicknesses

Number of Case Study	PM	Sleeve
1	2	1
2	2.5	1
3	3	1
4	2	1.5
5	2.5	1.5
6	3	1.5
7	2	2
8	2.5	2
9	3	2

factor, respectively. The rotor inner diameter (D_{ri}) can be expressed as [13]:

$$D_{ri}=D-2(g+h_m+T_{rc}) \tag{12}$$

The armature reaction inductance (L_m) is equal to 1.54^{mH} evaluated by [13]:

$$L_m=\frac{3}{\pi}\left(\left(k_{w1}N_c\right)/\left(p/2\right)\right)^2\times\left(\mu_0\times DL\right)/\left(g'K_c\right) \tag{13}$$

Both height of the stator slot wedge (H_{s1}) and the height of the stator tooth tip (H_{s0}) parameters cannot be calculated at the first step, so are assumed to be equal to 1^{mm} which is based on experience. So, the stator slot opening at the slot wedge (B_{s1}) is 11.02^{mm} owing to [13]:

$$B_{s1}=\pi\left(D+2\left(H_{s0}+H_{s1}\right)\right)/N_s-T_{sw} \tag{14}$$

The stator slot area per slot (A_s) is calculatable as 102.81^{mm2} by [13]:

$$A_s=\left(B_{s1}+B_{s2}\right)/2\times H_{s2}=102.81^{mm^2} \tag{15}$$

And, the end winding leakage inductance can be calculated by [13]:

$$L_{sle}=0.5\times pq\mu_0\left(T_{sw}+B_{s1}+B_{s2}/2\right)\left(3N_c/N_s\right)^2 \times\log\left(\left(T_{sw}+B_{s1}+B_{s2}/2\right)\sqrt{\pi}/\sqrt{2A_s}\right) \tag{16}$$

H_{s2} is the height of the stator from the wedge to the slot bottom, q is the number of slots per pole per phase, B_{s1} is the stator slot opening at the slot wedge, B_{s2} is the stator slot opening at the slot bottom, N_s is the number of stator slots. Another geometric parameter like the stator slot opening at the slot bottom ($B_{s2new}=13.19^{mm}$) and the height of stator from the wedge to the slot bottom ($H_{s2new}=13.63^{mm}$) are specified by [13]:

$$B_{s2new}=\left[\pi\left(D+2\left(H_{s0}+H_{s1}+H_{s2}\right)\right)/N_s\right]-T_{sw} \tag{17}$$

$$H_{s2new}=A_s/\left(\left(B_{s1}+B_{s2}\right)/2\right) \tag{18}$$

Finally, the current density (J_{snew}) is $3.93^{A/mm2}$ evaluated by [13]:

$$J_{snew}=J_s\times A_{cui}/A_{cu} \tag{19}$$

The stator outer diameter (D_o) is 133.26^{mm} as [13]:

$$D_o=D+2\left(H_{s0}+H_{s1}+H_{s2new}+T_{rc}\right) \tag{20}$$

According to the yield strength ($\sigma_{yield}=190^{MPa}$) and the expected maximum shaft torque (approximately equal to 4 times the rated torque) of the machine ($T_{max}=50.4^{N.m}$) and with respect to the safety factor of $n_s=50$, the frame thickness is 1.47^{mm} as [13]:

$$\frac{\pi}{2}\left(\left(\left(\frac{D_o}{2}\right)+t_f\right)^4-\left(\frac{D_o}{2}\right)^4\right)=\frac{(T_{\max}\times n_s\times\left(\frac{D_o}{2}\right)+t_f)}{\sigma_{yield}} \quad (21)$$

The calculated HS-PMSG volume and weights are stated in Table 2. At 15ºC, the copper resistivity is 2.52×10^{-8} Ωm so, the DC resistance (R_{DC}) is 0.05Ω and finally, the copper loss (P_{cu}) is 103.83W. The core loss (P_{core}) in the rated condition is *5289.6W*. Another loss such as the windage and the friction loss (P_{wf}) is assumed to be *200W* for a machine with this size and power is reasonable. The maximum flux density in the stator teeth (B_{st}) is calculated and is *1.09T*. In the steady-state, the permissible stator current regarding the PMs' demagnetization (I_{dmgrm}) is *124.56A*. The rated phase current (I_{ph}) is *26.31A* therefore, the PMs' demagnetization is not probable to occur.

3. MECHANICAL MODELING

The HS-PMSG rotor is assumed as a rotational cylinder and the inner stress is due to the radial ε_r and the tangential strains ε_θ. Concerning Hook's law and the isotropic and homogenous cylinder material assumptions, the radial strain ε_r can be calculated by [13]:

$$\varepsilon_r = 1/E_Y\left(\sigma_r-\upsilon\sigma_\theta\right)+\alpha_T\Delta T \quad (22)$$

where σ_r and σ_θ are the radial and tangential stress, E_Y and υ are young's modulus and Poisson's ratio respectively, α_T is the thermal expansion coefficient and ΔT is the variation between actual and reference temperatures and the tangential strain ε_θ is [13]:

$$\varepsilon_\theta = -\left(1/E_Y\right)\left(\upsilon\sigma_r+\sigma_\theta\right)+\alpha_T\Delta T \quad (23)$$

Equations (22) and (23) should satisfy the following equality [13]:

$$\sigma_r + r\left(d\sigma_r/dr\right)-\sigma_\theta+\rho\omega_m^2r^2=0 \quad (24)$$

TABLE 2. HS-PMSG weights and valume

Type	Weight (Kg) and Volume (m^3)
Stator Core	30.8
Stator tooth	5.68
Rotor Core	14.41
PMs (3^{mm})	3.42
Sleeve (2.85^{mm})	2.16
Windings	2.64
Frame	5.25
Total Weights	64.34
Total Volume	1500

where ω_m is the rotational speed and r is the radius of the infinitesimal portion of the cylinder with the mass density of ρ. The radial stress σ_r is accessible by solving the differential equation given by [13]:

$$\frac{d^2\sigma_r}{dr^2}+\frac{3d\sigma_r}{rdr}+(3+\upsilon)\rho\omega_m^2+(\frac{\alpha_T E_Y}{r})\frac{d\Delta T}{dr}=0 \quad (25)$$

The radial σ_r and the tangential σ_θ stresses play a role in Von Mises equivalent stress σ_{eq} defined as [13]:

$$\sigma_{eq}=\left(\sigma_r^2+\sigma_\theta^2-\sigma_r\sigma_\theta\right)^{1/2} \quad (26)$$

The values of mechanical parameters of the retention sleeve and the PM materials needed for the above equations are given in Table 3.

4. THICKNESS OF THE SLEEVE AND PM

The Taguchi optimization method is a statistical method developed by Genichi Taguchi for quality improvement, which is mostly employed in the engineering world. The objective functions are the thicknesses of the PM and the retentions sleeve. As been described, the aforementioned optimization method is implemented in MINITAB software which is an important software in this field. Hence, to avoid extending the optimization process, only the optimization results are given and these results are compared and optimized in the following sections. The orthogonal arrays (OA) reduce significantly the number of iterations and experiments of this optimization approach. In this algorithm, the ratio of Signal to Noise (S/N) is calculated by:

$$(S/N)_i=-10\log\left[\frac{1}{n}\sum_{j=1}^{n}\frac{1}{Y_{ij}^2}\right] \quad (27)$$

where i is the number of case studies and Y_{ij} is the measured value of quality for *i-th* and *j-th* case studies, and parameter n is the number of iterations for each case studies combination. The Taguchi optimization method often uses a two-step process. In the first stage, the (S/N) ratio is used to identify controlling factors to reduce changes. In the second stage, the control factors that have

TABLE 3. Mechanical Properties of the Sleeve and PM

Type	PM	Sleeve
Mass Density (g/mm^3)	0.0075	0.0045
Young Modulus (MPa)	170000	120000
Poisson Ratio (-)	0.24	0.34
Residual Magnetism (T)	1.37	-
Maximum Temperature (C)	80	-
Thermal Expansion Coefficient (10^{-6}/C)	4	9

a negligible effect on the (S/N) ratio are identified to achieve the goal. The response for each (S/N) ratio for any surface factor is Γ and ν. Γ is the difference between the maximum and minimum response (S/N ratio) for any factors and ν is each Γ rank. To using the optimization process, both the sleeve and the PM thicknesses are considered in Table 4. According to the Taguchi method the influences of PMs and sleeve on the sleeve centrifugal force **(State 1)**, on the PMs centrifugal force **(State 2)**, the maximum stress on the sleeve **(State 3)**, the maximum stress on the PMs **(State 4)**, the maximum strain on the sleeve **(State 5)**, the maximum strain on the PMs **(State 6)** all are given in Table 5. The Γ and ν changes according to Table 6.

5. RESULTS AND DISCUSSIONS

5. 2. Taguchi Optimization Method Results obtained from the Taguchi method is as : The sleeve thickness has a major impact on the sleeve centrifugal force, while the PM thickness has a minor influence. With an increase in PM thickness, the PM centrifugal force also increases, and the influence of the sleeve thickness is insignificant. The sleeve thickness affects the sleeve maximum stress directly via Γ while the PM thickness impresses the sleeve maximum stress up to 2.5mm. Variation of sleeve thickness from 1 to 2mm yields to 1.13% increase in the maximum stress of PM while the PM thickness varies from 2 to 3mm, the maximum stress in the PM rises 0.82%. It can be concluded that in comparison with PM thickness, the sleeve thickness variation has much influence on the maximum stress of the PM. For maximum strain in the sleeve, the impact of sleeve thickness is 10.25% more than the PM. From the sleeve thickness of 1 to 1.5mm, the maximum strain in PM decreases 2.28% and from 1.5 to 2mm increases 1.92% and for the PM thickness, from 2 to 2.5mm, the maximum strain in PM decreases 1.43% and from 2.5 to 3mm, increases 1.18%. So, the sleeve thickness has significant effects on the maximum strain of PM rather than the PM thickness.

In these 6 states, the thickness of the sleeve was the most important factor in calculating the centrifugal force in the sleeve, the maximum stress on the sleeve and the PM, and the maximum strain in the sleeve and the PM. The thickness of the sleeve is considered to be a vital factor.

5. 2. Electromagnetic Analysis According to Figures 3 and 4, the obtained results are as following: The maximum cogging torque from the 1st to 4th case study is constant and is 0.39N.m. It increases at the 9th case study, which has a maximum value of 1.23N.m. The increase in sleeve thickness does not affect the voltage of the HS-PMSG at the 1st to 3rd case study. This parameter increases 18.75% in the 4th case study and with a 47.37% increase, the maximum voltage becomes 227V. With a 31.11% increasing in the current of the HS-PMSG, the maximum value occurs in the 9th case study. The Joule loss in the 1st case study is 12.31W and with respect to

TABLE 5. The Effect of The Thicknesses of the Sleeve and PM on Various Parameters

Sleeve Thickness	PM Thickness	State 1	State 2	State 3	State 4	State 5	State 6
1	2	19.86	111.84	2746	3448	0.01583	0.0161
2	2.5	19.86	139.84	2806	3486	0.01595	0.01549
3	3	19.86	167.81	2861	3540	0.01635	0.01635
4	2	29.11	111.84	2803	3541	0.01613	0.01595
5	2.5	29.11	139.84	2929	3548	0.01637	0.0159
6	3	29.11	167.81	2808	3481	0.01649	0.01561
7	2	39.2	111.84	2849	3523	0.01647	0.01619
8	2.5	39.2	139.84	2877	3501	0.01618	0.01616
9	3	39.2	167.81	2915	3576	0.01665	0.01604

TABLE 6. (S/N) Ratio Resulted From Taguchi Method

Type	State 1		State 2		State 3		State 4		State 5		State 6	
	ST	PMT	ST	PMT	ST	PMT	ST	PMT	ST	PMT	ST	PMT
Γ	19.34	0	0	56	76	72	41	29	0.00039	0.00035	0.00037	0.00023
ν	1	2	2	1	1	2	1	2	1	2	1	2

ST = Seeve Thickness PMT = PM Thickness

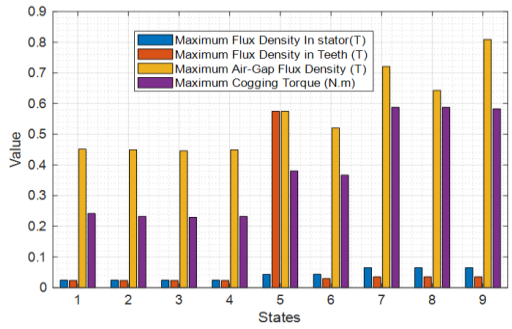

Figure 3. Changes on the maximum flux density in the stator, the maximum flux density in teeth, the maximum air-gap flux density, and the maximum cogging torque of HS-PMSG

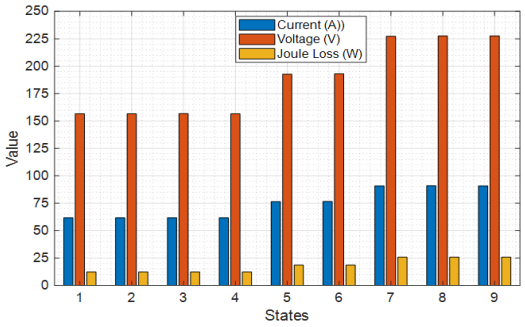

Figure 4. Changes in the stator current, the stator voltage, and the Joule loss of HS-PMSG

0.16% reduction, the minimum valve occurs in the 2nd, 3rd, and 4th case studies. For the maximum flux density in the teeth and the stator, from 1th to 4th case study, a state equal to 0.02T occurs. A maximum value for the maximum flux density in teeth occurs for the 5th case study. For the maximum flux density in the stator with a 68.75% increase, the maximum value takes place in the 9th case study. In this case study, the maximum flux density in teeth is equal to 0.5T. According to the results of the previous sections, the optimum thickness for the PM is *2.5mm* and for the retention sleeve is *2mm*.

6. FINAL DESIGN

One of the possible methods to find the proper and optimal thickness for the sleeve and the PM is to utilize the trial and error method. In this method, first, a set of various values for these two parameters is guessed. Then, various FEM analyses and simulations are performed to get closer to the optimal point. Obviously, this method is time-consuming and long. The proposed method in this manuscript is more accurate than the trial and error method and responds to variables faster. Another point that distinguishes the Taguchi optimization method is that in this method, the electromagnetic and mechanic variables affecting the performance of the HS-PMSG can be found and modified.

6. 1. Electromagnetic Design In this section, the electromagnetic design of HS-PMSG based on the above-discussed Taguchi optimization method has been accomplished. The electromagnetic design of the HS-PMSG is done using the JMAG that provides a variety of features to efficiently support optimized design. This is a popular and famous software among the designers of electrical machines and is mostly used in articles as design and simulation software. More, by using the JMAG, the results and sensitivity analysis offer functions where can improve the design. Figure 5 shows the HS-PMSG structure and geometrical property of HS-PMSG design is tabulated in Table 7. These parameters which are named geometric dimensions are based on the initial design of the HS-PMSG with respect to literature [13] which presented a design algorithm for PM machines. Due to a large number of equations in the design algorithm, only a number of them is described in the initial design of the HS-PMSG (Equations (1) to (21)) and others are categorized as Table 7. Figure 6 illustrates the FEM analysis of the HS-PMSG.

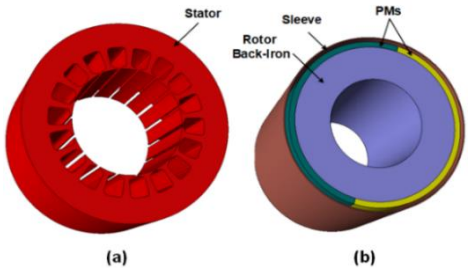

Figure 5. 3D-View of the designed HS-PMSG. a: stator, b: rotor

TABLE 7. Geometric Properties of HS-PMSG

Type	Value (mm)	Type	Value (mm)
Rotor Core Thickness	12.5	PM Thickness	2.5
Stator Core Thickness	12.5	Sleeve Thickness	1.5
Stator Teeth Width	3.11	Air-Gap	1
Slot Height	13.63	Stator Inner Diameter	76.31
Opening Slot	2	Stator Outer Diameter	132.26
Bottom Slot Length	11.02	Active Length	82
Top Slot Length	13.19	Frame Thickness	1.47
Shaft Radius	32	Wire Thickness	1.45

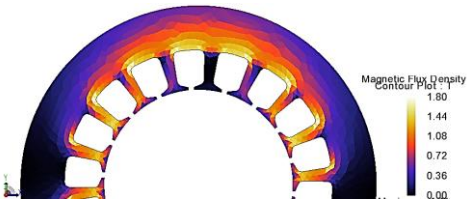

Figure 6. The no-load magnetic flux density of HS-PMSG

6. 2. Mechanical Design Figure 7 illustrates the 2-D view of the designed HS-PMSG rotor. Figure 8, displays the Von Mises stress and strain distribution on the HS-PMSG rotor. According to Figure 9, in the worst-case scenario, the amount of the Von Mises stress is equal to 682.167MPa in 60krpm. Similarly, for the Von Mises strain, the maximum value has been shown in Figure 10. The maximum shear stress of the titanium is equal to 729MPa. Therefore, for the worst condition in 60krpm, failure does not occur. Figure 11, shows the Hoop and radial stress in the sleeve. With a 0.5mm increasing, the Hoop and the radial stress increase 1.15 and 2.07%, responsively. The maximum valve occurs in 2mm which the Hoop stress is 277.19MPa and the radial stress is 275.05MPa. The maximum radial and the Hoop stress in PMs occurs in 1mm of the sleeve thickness that is equal to 355.34MPa and 337.42MPa, responsively. According to Figure 12, by 2.5mm increase in the thickness of PM, the radial stress is reduced by 0.55%, and also, the Hoop stress is reduced by 0.54%.

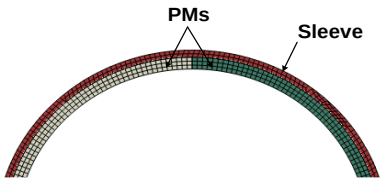

Figure 7. 2-D View of HS-PMSG rotor

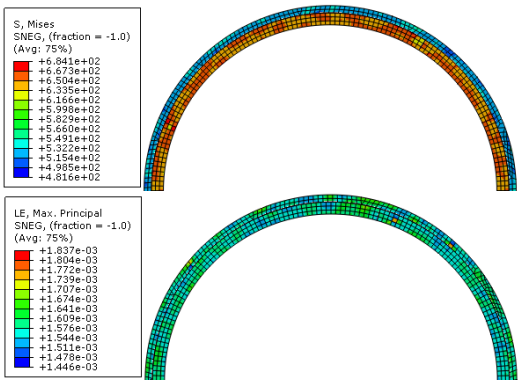

Figure 8. Von Mises stress (Top) and strain (Bottom) distribution on HS-PMSG rotor

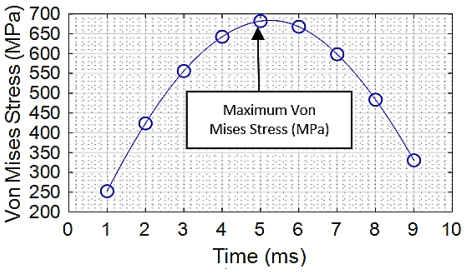

Figure 9. Maximum Von Mises stress

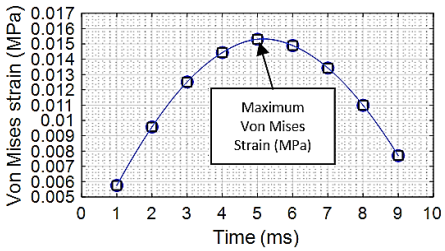

Figure 10. Maximum Von Mises strain

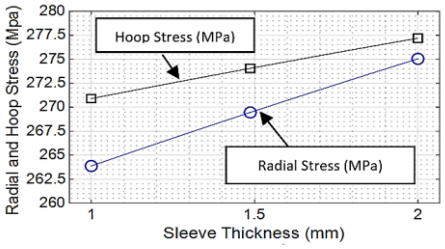

Figure 11. Sleeve's Hoop stress and the radial stress of PM

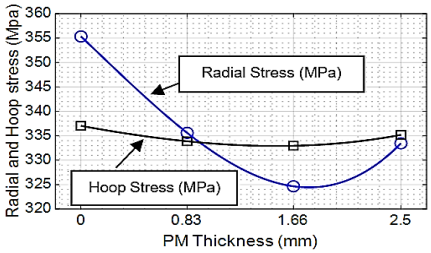

Figure 12. PM's Hoop stress and the radial stress of PM

7. CONCLUSION

In this paper, not only the proposed optimization method aims to improve the electromagnetic performance of the HS-PMSG but also the simulations sought to provide the proper mechanical conditions for the designed HS-PMSG. The result shows that: In the worst-case scenario of the rotational speed of 60krpm, the PM is safe against mechanical stresses and centrifugal forces. The Taguchi optimization method is utilized with a fast response to select the optimum thickness of the PM and the sleeve

and also, by utilizing the Taguchi optimization method, the cost reduction of the practical experiments and simulations is accessible. Compared with the initially designed HS-PMSG, in the optimum design, the following results are obtained: The cogging torque is reduced by 44.71%. The Joule loss is reduced by about 27.87%. The maximum flux density in teeth is reduced by approximately 37.5%. The PM and the sleeve weight are reduced 16.67 and 30.09% responsively, and the total weight of HS-PMSG is reduced by 2.78%.

8. REFERENCES

1. B. Poudel, E. Amiri, P. Rastgoufard and B. Mirafzal, "Toward Less Rare-Earth Permanent Magnet in Electric Machines: A Review," ***IEEE Transactions on Magnetics***, Vol. 57, No. 9, 1-19, (2021), DOI: 10.1109/TMAG.2021.3095615.
2. Tenconi, A., S. Vaschetto, and A.J.I.T.o.I.E. Vigliani, "Electrical machines for high-speed applications: Design considerations and tradeoffs", ***IEEE Transactions on Industrial Electronics***, Vol. 61, No. 6, (2013), 3022-3029, DOI: 10.1109/TIE.2013.2276769
3. H. Parivar, S. M. Seyyedbarzegar, A. Darabi, "An Improvement on Slot Configuration Structure of a Low-speed Surface-mounted Permanent Magnet Synchronous Generator with a Wound Cable Winding", ***International Journal of Engineering, Transactions C: Aspects***, Vol. 34, No. 9, (2021), 2045-2052, DOI: 10.5829/ije.2021.34.09c.01
4. Y. Gu, X. Wang, P. Gao and X. Li, "Mechanical Analysis With Thermal Effects for High-Speed Permanent-Magnet Synchronous Machines," ***IEEE Transactions on Industry Applications***, Vol. 57, No. 5, 4646-4656, (2021), DOI: 10.1109/TIA.2021.3087120.
5. R. Nasiri-Zarandi, A. Mohammadi Ajamloo, K. Abbaszadeh "Cogging Torque Minimization in Transverse Flux Permanent MagnetGenerators using Two-step Axial Permanent MagnetSegmentation for Direct Drive Wind Turbine Application", ***International Journal of Engineering, Transactions A: Basics,*** Vol. 34, No. 04, (2021), 908-918, DOI: 10.5829/ije.2021.34.04a.17
6. M. A. Rahman, "History of interior permanent magnet motors [History]," in ***IEEE Industry Applications Magazine,*** Vol. 19, No. 1, 10-15, (2013), DOI: 10.1109/MIAS.2012.2221996.
7. Z. Kolondzovski, a. Belahcen, and a. Arkkio, "Comparative thermal analysis of different rotor types for a high-speed permanent-magnet electrical machine,"***IET Electric Power Applications,*** Vol. 3, No. 4, 279-288, (2009). DOI: 10.1049/iet-epa.2008.0208
8. M. Arehpanahi, E.Kheiry, "A New Optimization of Segmented Interior Permanent Magnet Synchronous Motor Based on Increasing Flux Weakening Range and Output Torque" ***International Journal of Engineering, Transactions C: Aspects,*** Vol. 33, No. 6, (2020), 1122-1127, DOI: 10.5829/ije.2020.33.06c.09
9. T. Han, Y. Wang and J. -X. Shen, "Analysis and Experiment Method of Influence of Retaining Sleeve Structures and Materials on Rotor Eddy Current Loss in High-Speed PM Motors," ***IEEE Transactions on Industry Applications,*** Vol. 56, No. 5, (2020), 4889-4895, DOI: 10.1109/TIA.2020.3009909
10. Kurvinen E, Di C, Petrov I, Nerg J, Liukkonen O, Jastrzebski RP, Kepsu D, Jaatinen P, Aarniovuori L, Sikanen E, Pyrhonen J. "Design and Manufacturing of a Modular Low-Voltage Multi-Megawatt High-Speed Solid-Rotor Induction Motor." ***IEEE Transactions on Industry Applications,*** (2021), 1-10 DOI: 10.1109/TIA.2021.3084137
11. Q. Zhang, S. Cheng, D. Wang, Z. Jia, "Multiobjective design optimization of high-power circular winding brushless DC motor," ***IEEE Transactions Industrial Electronics***, Vol. 65, No. 2, (2018), 1740-1750, DOI: 10.1109/TIE.2017.2745456
12. Damiano, A. Floris, G. Fois, M. Porru and A. Serpi, "Modelling and design of PM retention sleeves for High-Speed PM Synchronous Machines," 2016 6th International Electric Drives Production Conference (EDPC), (2016), 118-125. DOI: 10.1109/EDPC.2016.7851323
13. K. M. G. Say, Performance and design of AC machines: Pitman, London, 1970, ISBN: 273 40199 8
14. Damiano, A. Floris, G. Fois, M. Porru and A. Serpi, "Modelling and design of PM retention sleeves for High-Speed PM Synchronous Machines," 2016 6th International Electric Drives Production Conference (EDPC), (2016), 118-125. DOI: 10.1109/EDPC.2016.7851323

9. APPENDIX

The proposed flowchart is as shown in Figure A1.

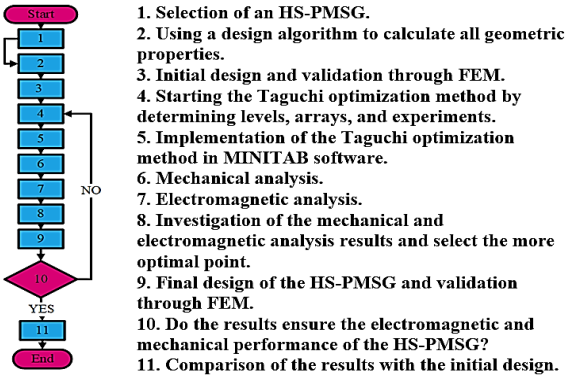

Figure A1. Proposed Flowchart

Persian Abstract

چکیده

در این مقاله، نویسندگان یک روش جدید برای طراحی ماشین سنکرون مغناطیس دائم سرعت بالا (HS-PMSG) مجهز به روکش محافظ ارائه داده اند. اهمیت استفاده از روکش محافظ زمانی حیاتی می‌شود که روتور در معرض تنش‌های شعاعی و مماسی ناشی از سرعت‌های بالا در حدود ۶۰ هزار دور بر دقیقه قرار می‌گیرد. با توجه به ویژگی‌های مکانیکی تیتانیوم، این ماده می‌تواند یک ماده مناسب برای استفاده در روکش HS-PMSG باشد. با استفاده از نظریه مکانیک الاستیگ، این ماده می‌تواند از نظر مکانیکی از روتور HS-PMSG محافظت کند. محور تحقیقات این مقاله بر روی طراحی الکترومغناطیسی و مکانیکی HS-PMSG که دارای ۲ قطب، ۱۸ شیار و توان ۴۰ کیلووات است متمرکز شده است. ماده آهنربای دائم استفاده شده در این ماشین NdFeB (نئودیمیوم) می‌باشد. نتایج بدست آمده با استفاده از دو نرم افزار JMAG و ABAQUS CAE می‌باشد که با استفاده از روش المان محدود اعتبار سنجی شده است. در بخش بعدی این مقاله، ضخامت‌های آهنربای دائم و روکش محافظ با استفاده از روش تاگوچی، بهینه‌سازی شده اند. نتایج بدست آمده از این روش پیشنهادی، عملکرد الکترومغناطیسی و مکانیکی HS-PMSG را در سرعت ۶۰ هزار دور بر دقیقه تضمین می‌کند و همچنین گشتاور دندانه‌ای، تلفات ژول، و وزن کلی HS-PMSG نسبت به طرح اولیه به ترتیب ۴۴.۷۱ درصد، ۲۷.۸۷ درصد و ۲.۷۸ درصد کاهش یافته‌اند.